Eur. Phys. J. B **58**, 361–365 (2007)
DOI: 10.1140/epjb/e2007-00239-7

THE EUROPEAN PHYSICAL JOURNAL B

Pressure-induced modifications of crystal and magnetic structure of oxygen deficient $La_{0.7}Sr_{0.3}MnO_{3-d}$ manganites

D.P. Kozlenko[1,a], S.V. Trukhanov[2], E.V. Lukin[1], I.O. Troyanchuk[2], and B.N. Savenko[1]

[1] Frank Laboratory of Neutron Physics, JINR, 141980 Dubna, Russia
[2] Joint Institute of Solids and Semiconductor Physics, NASB, P. Brovka str. 19, 220072, Minsk, Belarus

Received 28 May 2007
Published online 14 September 2007 – © EDP Sciences, Società Italiana di Fisica, Springer-Verlag 2007

Abstract. The crystal and magnetic structures of the oxygen deficient manganites $La_{0.7}Sr_{0.3}MnO_{3-d}$ (d = 0.15, 0.20) have been studied by means of powder neutron diffraction over the 0–5.2 GPa pressure and 10–290 K temperature ranges. $La_{0.7}Sr_{0.3}MnO_{2.85}$ exhibits a coexistence of rhombohedral ($R\bar{3}c$) and tetragonal ($I4/mcm$) crystal structures and below $T_g \sim 50$ K a spin glass state is formed. $La_{0.7}Sr_{0.3}MnO_{2.80}$ exhibits a tetragonal ($I4/mcm$) crystal structure. Below $T_g \sim 50$ K a phase separated magnetic state is formed, involving coexistence of C-type AFM domains with spin glass domains. In both compounds the crystal structure and magnetic states remain stable upon compression. The factors leading to the formation of different magnetic states in $La_{0.7}Sr_{0.3}MnO_{3-d}$ (d = 0.15, 0.20) and their specific high pressure behavior, contrasting with that of the stoichiometric $A_{0.5}Ba_{0.5}MnO_3$ (A = Nd, Sm) compounds showing pressure-induced suppression of the spin glass state and the appearance of the FM state, are analysed.

PACS. 62.50.+p High-pressure and shock wave effects in solids and liquids – 75.25.+z Spin arrangements in magnetically ordered materials – 75.47.Lx Manganites

1 Introduction

Perovskite-like manganites $A_{1-x}A'_xMnO_3$ (A-rare earth, A'-alkali earth elements) exhibit a rich variety of interesting physical phenomena which are at the current focus of extensive scientific investigations — colossal magnetoresistance, charge and orbital ordering, phase separation [1,2]. A complicated balance of the ferromagnetic (FM) double exchange mediated by delocalized e_g electrons and antiferromagnetic (AFM) superexchange between localized magnetic moments of t_{2g} nature coupled to lattice and orbital degrees of freedom leads to the formation of complex electronic and magnetic phase diagrams involving metallic and insulating ground states with various types of long range magnetic order, FM or AFM depending on particular types of A, A'-site elements and their ratio [1–4].

For the $0.2 < x < 0.5$ concentration range manganites generally exhibit a ferromagnetic metallic state below Curie temperature T_C due to the dominating role of the FM double exchange and the maximum values of T_C are reached for $x \sim 0.3$ [1,2]. The stoichiometric $La_{0.7}Sr_{0.3}MnO_3$ compound has $T_C \approx 370$ K, one of the largest values observed in manganites [3]. Recently it was shown that an introduction of relatively small concentration of oxygen vacancies leads to significant modification of the structural and magnetic properties of $La_{0.7}Sr_{0.3}MnO_{3-d}$ [4,5]. While the compounds with $0 < d < 0.15$ exhibit the rhombohedral crystal structure of $R\bar{3}c$ symmetry, for higher values $d \geqslant 0.15$ a formation of the new tetragonal phase of $I4/mcm$ symmetry and suppression of the FM metallic ground state in favor of the insulating spin glass (SG) state with $T_g \sim 50$ K was found. The characteristic feature of the SG state of $La_{0.7}Sr_{0.3}MnO_{3-d}$ is the presence of FM clusters with a size of about 10 nm embedded into the AFM matrix [6]. The investigation of the magnetization, susceptibility and heat capacity of $La_{0.7}Sr_{0.3}MnO_{2.85}$ at high pressures up to 1 GPa has revealed an increase of the volume part of the ferromagnetic clusters by about 5% [6].

The SG state formation was also found for stoichiometric compounds $A_{0.5}Ba_{0.5}MnO_3$ (A = Nd, Sm) with A-site cation disorder and large difference of ionic radius r_A [7]. At high pressures $P \sim 5$ GPa in $A_{0.5}Ba_{0.5}MnO_3$ (A = Nd, Sm) the appearance of the FM state and the suppression of the SG state occurs.

The observed increase of the volume part of the ferromagnetic clusters in $La_{0.7}Sr_{0.3}MnO_{3-d}$ at high pressures up to 1 GPa [6] implies that the FM state can be recovered at sufficiently high pressures, as it occurs in $A_{0.5}Ba_{0.5}MnO_3$ (A = Nd, Sm). One should note that the magnetic properties of $La_{0.7}Sr_{0.3}MnO_{3-d}$ were previously studied mostly by macroscopic methods (magnetization and susceptibility measurements), which can not exclude

[a] e-mail: denk@nf.jinr.ru

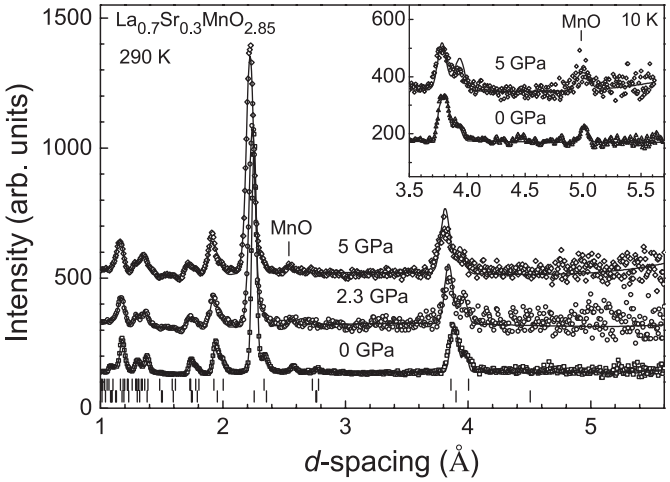

Fig. 1. Neutron diffraction patterns of $La_{0.7}Sr_{0.3}MnO_{2.85}$, measured at $P = 0$, 2.3 and 5 GPa, $T = 290$ and 10 K (inset) and processed by the Rietveld method. Experimental points and calculated profiles are shown. Ticks represent the calculated positions of nuclear peaks of rhombohedral (lower row) and tetragonal (upper row) phases. The positions of most intense nuclear and magnetic peaks of MnO impurity are also shown.

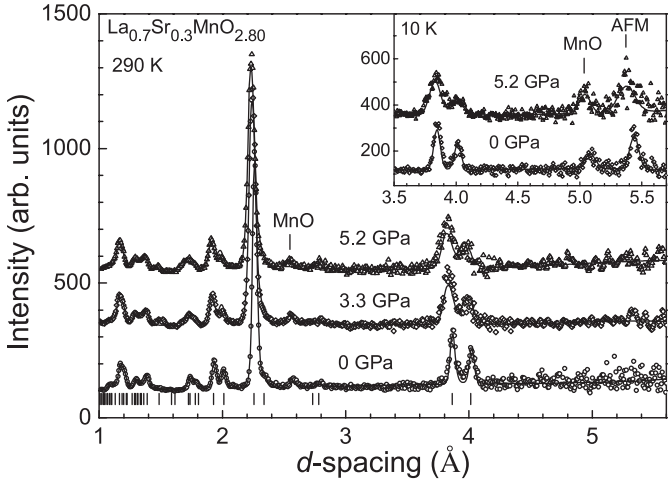

Fig. 2. Neutron diffraction patterns of $La_{0.7}Sr_{0.3}MnO_{2.80}$, measured at $P = 0, 3.3$ and 5.2 GPa, $T = 290$ and 10 K (inset) and processed by the Rietveld method. Experimental points and calculated profiles are shown. Ticks represent the calculated positions of nuclear peaks of tetragonal phase. The magnetic peak (100) of C-type AFM phase is marked as "AFM". The positions of most intense nuclear and magnetic peaks of MnO impurity are also shown.

unambiguously the possibility of the coexistence of SG state and long range ordered magnetic state. Additional insight into the nature of magnetic state and relationship of its features with structural parameters can be obtained from neutron diffraction measurements. In this paper, the crystal and magnetic structure of $La_{0.7}Sr_{0.3}MnO_{3-d}$ ($d = 0.15$, 0.2) are studied by means of powder neutron diffraction at high pressures up to 5.2 GPa.

2 Experimental

The synthesis procedure of $La_{0.7}Sr_{0.3}MnO_{3-d}$ ($d = 0.15$, 0.2) is described in [4]. The oxygen content value was determined by thermogravimetric method with an accuracy of 0.01.

Neutron powder diffraction measurements at high pressures up to 5.2 GPa in the low temperature range 10–290 K were performed with the DN-12 diffractometer [8] at the IBR-2 high flux pulsed reactor (FLNP JINR, Dubna, Russia) using a sapphire anvil pressure cells [9]. The sample volume was about 2 mm^3. The pressure was determined by the ruby fluorescence technique. Diffraction patterns were collected at the scattering angle $2\theta = 90°$ with the resolution $\Delta d/d \approx 0.015$.

Experimental data were analysed by the Rietveld method using the MRIA program [10] or Fullprof [11] if magnetic structure was to be included.

3 Results and discussion

Neutron diffraction patterns of $La_{0.7}Sr_{0.3}MnO_{2.85}$ and $La_{0.7}Sr_{0.3}MnO_{2.80}$ measured at selected pressures and temperatures and processed by the Rietveld method are shown in Figures 1 and 2. A small impurity of MnO (about 5%) was found in both samples. For the stoichiometric $La_{0.7}Sr_{0.3}MnO_3$ compound with the rhombohedral crystal structure of $R\bar{3}c$ symmetry at $d \sim 3.9$ and 1.95 Å only single peaks (012) and (024) (in hexagonal setting) are expected to appear [12]. The observed splitting of the diffraction peaks at these d-spacings (Figs. 1 and 2) corresponds to the appearance of the new phase with lower crystal structure symmetry.

After the Rietveld analysis of the experimental data it was found that there is a coexistence of the rhombohedral ($R\bar{3}c$) and tetragonal ($I4/mcm$) phases in $La_{0.7}Sr_{0.3}MnO_{2.85}$ with volume fractions of 40 and 60%, respectively. Such phase coexistence was also observed in the previous study of a sample with similar oxygen content at ambient conditions. It was assumed to be related to the clusterization of oxygen vacancies [5].

Upon cooling at $T < T_g \sim 50$ K in $La_{0.7}Sr_{0.3}MnO_{2.85}$ we observed neither appearance of the additional contribution to nuclear peaks intensity, characteristic for ferromagnetism, nor appearance of new magnetic peaks at high pressures up to 5 GPa (Fig. 1). Such an observation is consistent with the formation of the SG state without long range magnetic order and its stability in the investigated pressure range. The similar character of the diffraction patterns indicates the absence of structural transformations and a weak dependence of volume fractions of the rhombohedral and tetragonal phases of $La_{0.7}Sr_{0.3}MnO_{2.85}$ in the investigated temperature and pressure ranges.

The diffraction patterns of $La_{0.7}Sr_{0.3}MnO_{2.80}$ exhibit more pronounced splitting of the diffraction peaks at $d \sim 3.9$ and 1.95 Å (Fig. 2) and they correspond to the pure tetragonal $I4/mcm$ phase in the studied pressure

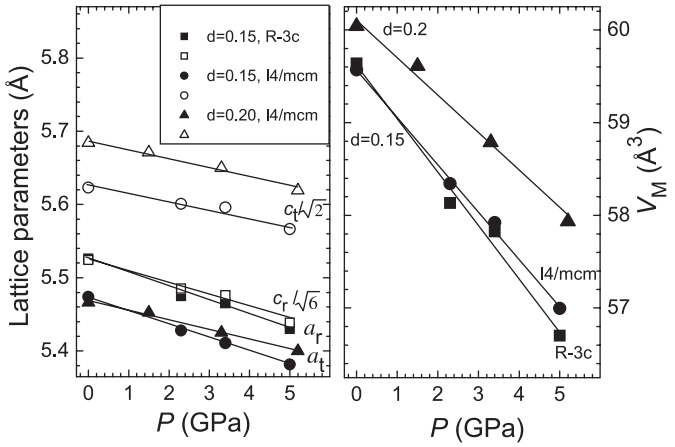

Fig. 3. Pressure dependencies of lattice parameters (left panel) and unit cell volume per formula unit (right panel) of rhombohedral (in hexagonal setting) and tetragonal phases of $La_{0.7}Sr_{0.3}MnO_{2.85}$ and $La_{0.7}Sr_{0.3}MnO_{2.80}$, fitted by linear functions and Birch-Murnaghan EOS, respectively.

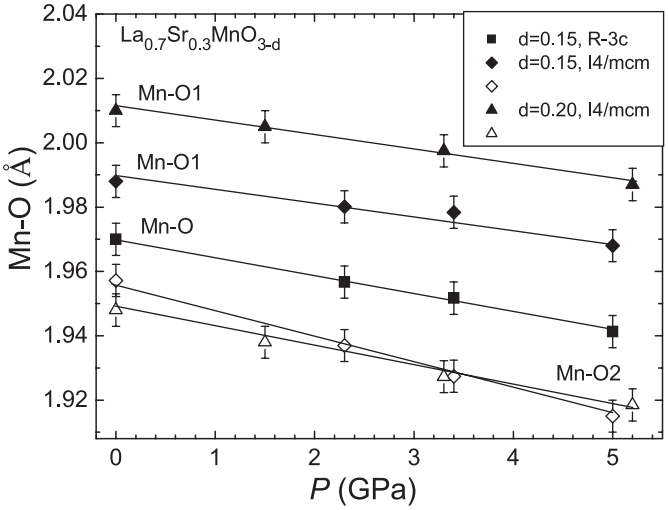

Fig. 4. Pressure dependencies of Mn-O bond lengths of rhombohedral and tetragonal phases of $La_{0.7}Sr_{0.3}MnO_{2.85}$ and $La_{0.7}Sr_{0.3}MnO_{2.80}$, fitted by linear functions.

range up to 5.2 GPa, as found from the Rietveld analysis of the data. At $T < T_g \sim 50$ K the appearance of the new magnetic peaks (100) and (102) at $d = 5.43$ and 3.22 Å was observed while no additional contribution to nuclear peaks intensity occurs (Fig. 2). Such an observation corresponds to the formation of the C-type AFM state [13–16]. In this AFM state manganese moments form ferromagnetic chains along the tetragonal c-axis with antiferromagnetic coupling between neighbouring chains and its characteristic feature is the $d(3z^2-r^2)$ e_g orbital polarization [13–15]. The obtained value of the ordered manganese magnetic moment at ambient pressure and $T = 10$ K is $\mu = 1.4(1)$ μ_B and it is considerably less than the expected one of 4.1 μ_B for the fully long range ordered magnetic state. The small μ value implies the presence of magnetic phase separation due to a coexistence of the C-type AFM domains with short range ordered SG regions, presumably of nanoscopic (or mesoscopic) size and total volume fractions of these phases about 15 and 85%. With increasing pressure up to 5.2 GPa the μ value increases slightly up to 1.6 (1) μ_B, indicating the possible growing of the C-type AFM phase volume.

In the rhombohedral phase of $La_{0.7}Sr_{0.3}MnO_{2.85}$ oxygen atoms are located in positions 18(e) (x, 0, 0.25) (in hexagonal setting) with $x \sim 0.450$ and MnO_6 octahedra are isotropic with equal values of Mn-O bond lengths and Mn-O-Mn bond angles [5,12]. The lattice parameters, unit cell volume and Mn-O bond lengths decrease nearly linearly under pressure (Figs. 3 and 4). Their values obtained at ambient pressure are similar to those of previous studies [5,16]. The calculated linear compressibilities $k_{li} = -(1/(l_i)_{P=0})(dl_i/dP)_T$ ($l_i = a$, c, $l_{\mathrm{Mn-O}}$) at ambient temperature are 0.0034, 0.0030 and 0.0029 GPa^{-1} for the a, c lattice parameters and Mn-O bond length, respectively. The Mn-O-Mn bond angle varies slightly from 165.1 to 163.4° in the 0–5 GPa pressure range. The bulk modulus value $B_0 = -V(dP/dV)_T = 95(5)$ GPa calculated from the fitting of the volume compressibility data (Fig. 3) by the Birch-Murnaghan equation of state [17] with its pressure derivative $B' = (dB_0/dP)_T = 4$ is much lower than $B_0 = 167$ GPa found for the stoichiometric $La_{0.7}Sr_{0.3}MnO_3$ [12].

In the tetragonal phase of $La_{0.7}Sr_{0.3}MnO_{2.85}$ and $La_{0.7}Sr_{0.3}MnO_{2.80}$ oxygen atoms are located in positions O1 – 4(a) (0, 0, 0.25) and O2–8(h) (x, $1/2 + x$, 0) with $x \sim 0.782$ [5,16]. There are two non-equivalent types of Mn-O bond distances — Mn-O1, oriented along the c-axis and Mn-O2 lying in the ab plane. Due to a larger Mn-O1 value in comparison with Mn-O2 one (Fig. 4), MnO_6 octahedra are apically elongated with respect to the c-axis. The lattice parameters, unit cell volume and Mn-O1,2 bond lengths also decrease nearly linearly under pressure (Figs. 3 and 4) and their values obtained at ambient pressure are similar to those found in previous studies [5,16]. The lattice compression of the tetragonal phase of $La_{0.7}Sr_{0.3}MnO_{2.85}$ is anisotropic with the most compressible a-axis. The calculated linear compressibilities are $k_a = 0.0034$ and $k_c = 0.0019$ GPa^{-1} for the a and c axes and $k_{\mathrm{Mn-O2}} = 0.0043$ and $k_{\mathrm{Mn-O1}} = 0.0019$ GPa^{-1} for the Mn-O2 and Mn-O1 bonds. For $La_{0.7}Sr_{0.3}MnO_{2.80}$ the compression anisotropy is less pronounced with linear compressibility values $k_a = 0.0024$ and $k_c = 0.0022$ GPa^{-1} for the a and c axes and $k_{\mathrm{Mn-O2}} = 0.0029$ and $k_{\mathrm{Mn-O1}} = 0.0022$ GPa^{-1} for the Mn-O2 and Mn-O1 bonds. The bulk modulus values $B_0 = 108(5)$ and 140(5) GPa obtained for the tetragonal phase of $La_{0.7}Sr_{0.3}MnO_{2.85}$ and $La_{0.7}Sr_{0.3}MnO_{2.80}$ with $B' = 4$ are also smaller than one 167 GPa for stoichiometric $La_{0.7}Sr_{0.3}MnO_3$ [12], although larger than $B_0 = 95$ GPa for the rhombohedral phase of $La_{0.7}Sr_{0.3}MnO_{2.85}$. The decrease of bulk modulus in oxygen deficient compounds can be related to their lower atomic density. The Mn-O2-Mn bond angle increases from 162.9 to 166.9° in the 0–5 GPa pressure range for $La_{0.7}Sr_{0.3}MnO_{2.85}$ and it

increases from 165.7 to 168.7° in the 0–5.2 GPa pressure range for $La_{0.7}Sr_{0.3}MnO_{2.80}$. The Mn-O1-Mn bond angle is equal to 180°.

The drastic difference between magnetic states of $La_{0.7}Sr_{0.3}MnO_{2.85}$ and $La_{0.7}Sr_{0.3}MnO_{2.80}$ is closely related to their structural features and chemical content. In $La_{0.7}Sr_{0.3}MnO_{2.85}$ ($La^{3+}_{0.7}Sr^{2+}_{0.3}Mn^{3+}_{1}O^{2-}_{2.85}$) there is a considerable amount of the rhombohedral phase with isotropic MnO_6 octahedra, oxygen vacancies distribution and e_g orbital polarization. For this case the superexchange interactions Mn^{3+}-$O^{2-}Mn^{3+}$ are ferromagnetic for the octahedral coordination of Mn ions and antiferromagnetic for the pentahedral one in the vicinity of oxygen vacancies [4,5]. The competing balance of these interactions is assumed to be a driving force for the formation of the SG state in $La_{0.7}Sr_{0.3}MnO_{3-d}$ [4,5].

The $La_{0.7}Sr_{0.3}MnO_{2.80}$ ($La^{3+}_{0.7}Sr^{2+}_{0.3}Mn^{3+}_{0.9}Mn^{2+}_{0.1}O^{2-}_{2.8}$) compound has the tetragonal crystal structure and two types of Mn ions, Mn^{3+} (90%) and Mn^{2+} (10%). The apical elongation of MnO_6 octahedra leads to the preferential population of $d(3z^2 - r^2)$ e_g orbitals oriented along the c-axis, creating favourable conditions for the appearance of the C-type AFM state [13–15]. The oxygen vacancies occupy preferentially O2 – 8(h) (x, $1/2 + x$, 0) positions [5]. This factor along with the $d(3z^2 - r^2)$ e_g orbital polarization lead to the FM character of Mn^{3+}-O^{2-}-Mn^{2+} interactions along the c-axis and AFM character of Mn^{3+}-O^{2-}-Mn^{2+} and Mn^{3+}-$O^{2-}Mn^{3+}$ interactions in both octahedral and pentahedral coordination of Mn ions. Therefore, the frustration of magnetic interactions for the tetragonal structure of $La_{0.7}Sr_{0.3}MnO_{2.80}$ is substantially reduced in comparison with the rhombohedral phase of $La_{0.7}Sr_{0.3}MnO_{2.85}$, leading to the appearance of the C-type AFM state domains.

Although $La_{0.7}Sr_{0.3}MnO_{2.85}$ also exhibits a fraction of tetragonal phase, no appearance of magnetic peaks characteristic for the C-type AFM state was observed. It implies that coexistence of tetragonal and rhombohedral phases increases the frustration effects, leading to suppression of AFM state fraction expected for the tetragonal phase in the favor of SG one.

Apart from oxygen deficient $La_{0.7}Sr_{0.3}MnO_{3-d}$, the spin glass state was also observed in stoichiometric $A_{0.5}Ba_{0.5}MnO_3$ (A = Nd, Sm) compounds with disorder and large size difference of A-site cation [7]. In this case the application of high pressures $P \sim 5$ GPa leads to the suppression of the SG state and appearance of the FM state. In $A_{0.5}Ba_{0.5}MnO_3$ ($A^{3+}_{0.5}Ba^{2+}_{0.5}Mn^{3+}_{0.5}Mn^{4+}_{0.5}O^{2-}_{3}$) the formation of the SG state is due to the competing balance between FM double exchange and AFM superexchange interactions, coupled with the positional disorder in the A-site sublattice. At high pressures a reduction of the Mn-O bond distances and increase of Mn-O-Mn bond angles values occur, shifting the balance of competing interactions in the favour of the FM double exchange one.

It is reasonable to assume the formation of FM state in manganites with initial SG state under pressure occurs by growing and conglomeration of FM clusters imbedded into AFM matrix [4,5]. In contrast to stoichiometric manganites, in oxygen deficient manganites principal restrictions on the maximal size of FM clusters exist, since in the vicinity of oxygen vacancies the magnetic interactions between the neighboring clusters are weak due to the large Mn-Mn distance ∼3.9 Å and negligible strength of direct exchange. For the vacancies concentration $d \sim 0.15$–0.2 they should appear with non-negligible probability even in first and second coordination shells around Mn ions, which contain 6 and 16 O ions. For the isotropic vacancies distribution characteristic for the rhombohedral phase of $La_{0.7}Sr_{0.3}MnO_{2.85}$, within more distant coordination shells it will be enough oxygen vacancies to prevent the growing of the FM cluster. The characteristic cluster size is ∼10 nm [6], which is equivalent to about 30 Mn-O-Mn distances. The increase of the volume fraction of FM clusters at high pressures up to 1 GPa found for $La_{0.7}Sr_{0.3}MnO_{2.85}$ [6] can be explained by the pressure-induced enhancement of FM superexchange interactions and some increase of FM clusters size up to possible maximum one, limited by the local geometry of oxygen vacancies distribution.

For $La_{0.7}Sr_{0.3}MnO_{2.80}$ with tetragonal crystal structure the spatial distribution of oxygen vacancies is anisotropic and they are located preferentially in the ab planes. This creates favorable conditions for the formation of more extended AFM domains along the c-axis in comparison with the characteristic size of FM clusters for the rhombohedral phase.

4 Conclusions

The results of our study show that the spin glass state is formed in oxygen deficient compound $La_{0.7}Sr_{0.3}MnO_{2.85}$ containing Mn^{3+} ions only and exhibiting the coexistence of rhombohedral and tetragonal structure. In $La_{0.7}Sr_{0.3}MnO_{2.80}$ with tetragonal structure and two different types of Mn ions, Mn^{3+} and Mn^{2+}, a coexistence of the long range ordered C-type AFM domains and short range ordered SG regions occur, presumably at nanoscopic or mesoscopic scale. The difference in the magnetic state of $La_{0.7}Sr_{0.3}MnO_{2.85}$ and $La_{0.7}Sr_{0.3}MnO_{2.80}$ comes from peculiarities of structural properties, magnetic interactions, orbital polarization and oxygen vacancies distribution in these compounds.

The magnetic states of $La_{0.7}Sr_{0.3}MnO_{2.85}$ and $La_{0.7}Sr_{0.3}MnO_{2.80}$ remain stable in the investigated pressure range and no appearance of the ferromagnetism occurs, in opposite to the case of stoichiometric $A_{0.5}Ba_{0.5}MnO_3$ (A = Nd, Sm) compounds, also exhibiting initial spin glass state. The topological factor related to the oxygen vacancies distribution creates additional restrictions on the possible maximal size of FM clusters imbedded into AFM matrix of the SG state, preventing the development of the long range ordered FM state.

The work is supported by Russian Foundation for Basic Research and Belarusian Republican Foundation for Fundamental Research, grants 06-02-81018-Bel-à and F06P–078.

References

1. E. Dagotto, T. Hotta, A. Moreo, Phys. Rep. **344**, 1 (2001)
2. M.B. Salamon, M. Jaime, Rev. Modern Phys. **73**, 583 (2001)
3. A. Urushibara, Y. Moritomo, T. Arima, A. Asamitsu, G. Kido, Y. Tokura, Phys. Rev. B **51**, 14103 (1995)
4. S.V. Trukhanov, JETP **100**, 95 (2005)
5. S.V. Trukhanov, I.O. Troyanchuk, A.V. Trukhanov, I.A. Bobrikov, V.G. Simkin, A.M. Balagurov, JETP Lett. **84**, 254 (2006)
6. S.V. Trukhanov, I.O. Troyanchuk, A.V. Trukhanov, I.M. Fita, A.N. Vasil'ev, A. Maignan, H. Szymczak, JETP Lett. **83**, 33 (2006)
7. N. Takeshita, C. Terakura, D. Akahoshi, Y. Tokura, H. Takagi, Phys. Rev. B **69**, 180405 (2004)
8. V.L. Aksenov, A.M. Balagurov, V.P. Glazkov, D.P. Kozlenko, I.V. Naumov, B.N. Savenko, D.V. Sheptyakov, V.A. Somenkov, A.P. Bulkin, V.A. Kudryashev, V.A. Trounov, Physica B **265**, 258 (1999)
9. V.P. Glazkov, I.N. Goncharenko, High Pressure Physics and Techniques **1**, 56 (in Russian) (1991)
10. V.B. Zlokazov, V.V. Chernyshev, J. Appl. Cryst. **25**, 447 (1992)
11. J. Rodriguez-Carvajal, Physica B **192**, 55 (1993)
12. D.P. Kozlenko, I.N. Goncharenko, B.N. Savenko, V.I. Voronin, J. Phys.: Condens. Matter **16**, 6755 (2004)
13. D.P. Kozlenko, V.P. Glazkov, Z. Jirák, B.N. Savenko, J. Phys.: Condens. Matter **16**, 2381 (2004)
14. R. Kajimoto, H. Yoshizawa, H. Kawano, Y. Tokura, K. Ohoyama, M. Ohashi, Phys. Rev. B **60**, 9506 (1999)
15. Z. Fang, I.V. Solovyev, K. Terakura, Phys. Rev. Lett. **84**, 3169 (2000)
16. D.P. Kozlenko, S.V. Trukhanov, E.V. Lukin, I.O. Troyanchuk, B.N. Savenko, V.P. Glazkov, JETP Lett. **85**, 113 (2007)
17. F.J. Birch, J. Geophys. Res. **91**, 4949 (1986)